

Evidence for nuclear shape coexistence at $N = 88$: $^{152}\text{Eu}(d,p)$ and (d,t) reactions

Robert G. Lanier, Gordon L. Struble, Lloyd G. Mann, and Ivan C. Oelrich*
Nuclear Chemistry Division, Lawrence Livermore Laboratory, Livermore, California 94550

Ivan D. Proctor and Dale W. Heikkinen
Experimental Physics Division, Lawrence Livermore Laboratory, Livermore, California 94550
 (Received 30 November 1979)

The (d,p) and (d,t) reactions on an isotopically enriched radioactive target of ^{152}Eu were investigated at a deuteron bombarding energy of 20 MeV. The triton spectrum showed the following features: (1) levels in ^{151}Eu below ~ 260 keV were virtually unpopulated, (2) the pickup strength of one-quasiparticle states is severely fragmented and is spread over a group of levels between ~ 260 and ~ 950 keV, and (3) the majority of the pickup strength is concentrated in a narrow band of levels between ~ 2.3 and ~ 2.8 MeV. An analysis of these data in conjunction with other available information on the structure of ^{151}Eu suggests the coexistence of three distinct shapes in ^{151}Eu : states related to the ground state are spherical, states related to a $5/2^+$ state at 260 keV are moderately deformed, and states between ~ 2.3 and ~ 2.8 MeV are strongly deformed and are essentially one-neutron holes coupled to a two-quasiparticle configuration which is identical to the ground state structure of ^{152}Eu . The spectrum observed in the (d,p) reaction shows that the ^{153}Eu $5/2^+$ ground state rotational band is weakly populated to $I = 11/2$, but shows few other states below ~ 2 MeV. The intensity patterns and angular distributions for the ^{153}Eu ground band are consistent with pure $l = 5$ transfer to the ^{152}Eu $\{\pi 5/2[413], \nu 11/2[505]\}_{\kappa=3}$ ground state.

NUCLEAR REACTIONS $^{152}\text{Eu}(d,p)$ and (d,t) with isotopically enriched radioactive target; $E_d = 20$ MeV; measured E_p , E_t , and $\sigma(\theta)$ with Q3D spectrograph; DWBA analysis, deduced levels, J^π .
 NUCLEAR STRUCTURE ^{151}Eu and ^{153}Eu assigned Nilsson configurations; shape coexistence in ^{151}Eu .

I. INTRODUCTION

Experimental work which has focused on determining shape coexistence in light rare-earth nuclei has been extensively published. A number of authors¹⁻⁵ have speculated about coexistence in the even-even nuclei around $N = 90$, because the (p,t) and (t,p) $l = 0$ strength is fragmented over several 0^+ states in a manner which is interpreted as being consistent with shape coexistence. Similar studies bearing on the problems of shape coexistence in odd- A nuclei have also been done.⁶⁻⁸ Using γ -ray spectroscopy, Kleinheinz *et al.*⁹ reported shape coexistence in ^{151}Gd . They observed a rotational band with a very small deformation based on the $i_{13/2}$ orbital and a strongly deformed band up to $I = \frac{25}{2}$ built on the $h_{11/2}$ orbital. Using the same experimental technique, Cook *et al.*¹⁰ also observed a well-developed $h_{11/2}$ rotational structure in ^{151}Sm .

Shape coexistence has been postulated^{6,7} for ^{151}Eu in particular. Some experimental data closely related to this question are shown¹¹ in Fig. 1. The earliest work involved measurements of Coulomb excitation¹² and inelastic scattering,¹³ and these data were interpreted in terms of phonon excitations coupled to a $(d_{5/2})^{-1}$ [or $(d_{5/2})$] ground state. States strongly populated in the $(^3\text{He}, d)$ reaction^{14,15} suggested further spherical structures

involving the $g_{7/2}$ and probably the $h_{11/2}$ proton (or proton holes) coupled to a ^{150}Sm (or ^{152}Gd) ground state.^{16,17} In (p,t) reaction studies,^{6,7} the states considered to have spherical structures were weakly populated and an additional set of states, starting with a $\frac{5}{2}^+$ level at 260 keV, were strongly populated. The authors postulated that this level is the band head of the $\frac{5}{2} [413]$ intrinsic Nilsson state.¹⁸ They also suggested that the level at 415 keV was a $\frac{7}{2}^+$ rotational band member and further interpreted levels at 654 and 801 keV as the $\frac{5}{2}^+$ and $\frac{7}{2}^+$ members of the β -vibrational band built on the $\frac{5}{2} [413]$ orbital. Subsequent in-beam γ -ray experiments by Taketani *et al.*¹⁹ identified additional members of the deformed $\frac{5}{2} [413]$ band up to $I = \frac{11}{2}$ and determined an average rotational parameter of $\hbar^2/2\mathcal{I} = 21.6$ keV for the band. All of these experimental data, some of which are summarized in Fig. 1, are consistent with the notion that spherical and deformed structures coexist in ^{151}Eu and that inelastic scattering and the $(^3\text{He}, d)$ reaction selectively populate spherical states while the (p,t) reaction preferentially populates deformed states.

Although a spherical structure appears reasonable for the ^{151}Eu ground state and for some of the higher-lying positive parity states, calculations by Sen,²⁰ and detailed comparisons of these

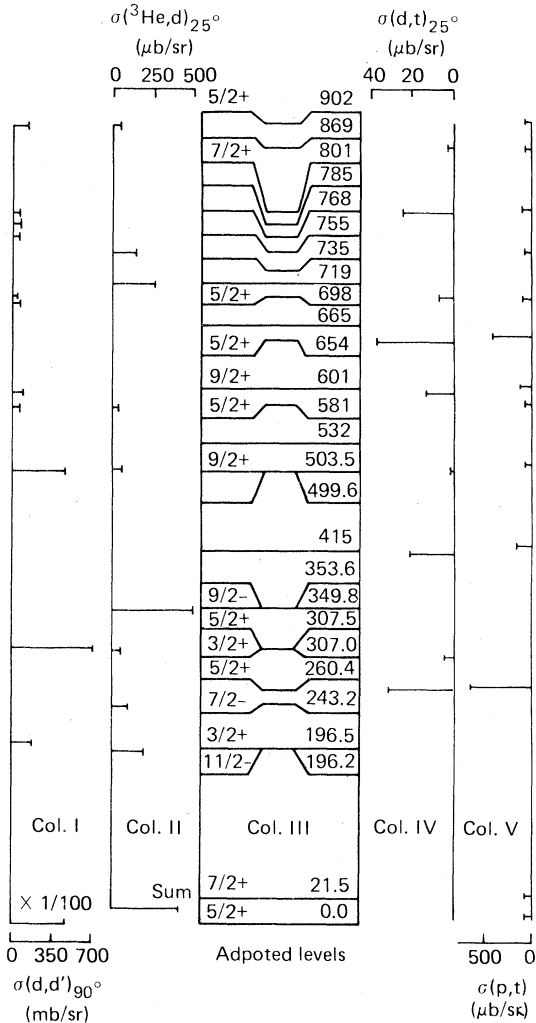


FIG. 1. Experimental data below 1 MeV for ^{151}Eu . The data displayed from left to right are (I) inelastic deuteron scattering, (II) the $^3\text{He}, d$ reaction, (III) adopted levels from Nuclear Data Sheets (Ref. 11), (IV) our experimental data at 25° , and (V) the (p, t) results.

calculations by Dracoulis and Leigh with their experimental results,^{21,22} suggest apparently conflicting possibilities.²³ Sen calculated the low-lying positive parity levels by coupling single proton-hole motion in the $2d_{5/2}$ and $1g_{7/2}$ orbitals to the quadrupole vibrations of the ^{152}Gd core. He found that the energy levels and $B(E2)$ values are reproduced reasonably well but the calculated and experimental spin assignments of some of the levels were in serious disagreement. The subsequent experiments by Dracoulis and Leigh considerably improved the agreement with Sen's results, but other problems, such as the failure to predict the observed low-lying $\frac{3}{2}^+$ state at ~ 196 keV, were apparent in the comparison. Moreover, the experimental data showed the existence

of a decoupled band (~ 196 keV) built on the $h_{11/2}$ orbital, and this is consistent with expectations for a nucleus with a small deformation if Coriolis effects are included. Prompted by this observation, Dracoulis and Leigh²³ performed a Coriolis-mixing calculation and attempted to describe the low-lying positive parity states and the states of the decoupled band in terms of mixtures of weakly deformed Nilsson states. By introducing different quadrupole deformations for the Nilsson orbitals derived from the $g_{7/2}(\beta_2=0.16)$, $h_{11/2}(0.16)$, and $d_{5/2}(0.11)$ spherical states, they obtain a relatively consistent description of the $\frac{1}{2}^-$ decoupled band and for many of the features of the low-lying positive parity states as well. However, their model does not yield, for example, sufficient fragmentation of the $B(E2)$ strength among the observed $\frac{3}{2}^+$ states and fails to account for the $B(E2)$ value ($3 \pm 1 \times 10^{-4} e^2 b^2$) of the 260-keV "deformed" state by several orders of magnitude.²²

In view of the conflicting interpretations of the low-lying levels of ^{151}Eu and the relation of these states to the question of shape coexistence, we performed (d, t) and (d, p) reaction studies on a specially fabricated target²⁴ of ^{152}Eu . Some of these results²⁵ as well as other studies related to the characterization of the nuclear structure of the target state^{26,27} have been reported previously.

II. EXPERIMENTAL PROCEDURE

The experiments were performed using a beam of 20-MeV deuterons from the three-stage tandem Van de Graaff facility at the Los Alamos Scientific Laboratory. We obtained energy spectra for the protons and tritons with a quadrupole-triple-dipole (Q3D) spectrograph.²⁸ The particles were detected with a 1-m-long, helical proportional counter mounted on the focal plane of the magnet. A number of enriched targets of radioactive ^{152}Eu were obtained by mass separating a chemically purified sample of enriched $^{151}\text{Eu}_2\text{O}_3$ that had undergone neutron irradiation at the Oak Ridge high-flux reactor. Each target was supported on an ~ 50 - $\mu\text{g}/\text{cm}^2$ carbon substrate and had a thickness of ~ 40 $\mu\text{g}/\text{cm}^2$. The details describing the preparation of the radioactive target have been published elsewhere.²⁴

An energy calibration for the spectrometer was obtained for both the (d, t) and (d, p) reactions. The calibration reactions were $^{167}\text{Er}(d, t)$ and $^{182}\text{W}(d, p)$. Energy values for the strongly populated states were taken from published compilations.^{29,30} Triton spectra from the $^{152}\text{Eu}(d, t)$ reaction were measured in 10° intervals between 15° and 65° . The spectra from the $^{152}\text{Eu}(d, p)$ reaction were also taken in 10° steps but the angular range was limited to between 25° and 65° . The energy bite

accepted by the spectrograph detector was ~ 1.5 MeV and the accumulated counts were stored in a 2048-channel array. For both reactions, two and sometimes three overlapping energy bites were taken to cover the full excitation energy range up to ~ 3 MeV. The reaction yield data were corrected for dead-time losses, and the data recorded at different scattering angles were normalized to the number of elastic scattering events counted in a solid-state detector placed at 30° with respect to the beam. The absolute cross sections were derived by normalizing the monitor elastic yields to optical model calculations (see Table III) and by using the known ratio of monitor and spectrograph efficiencies. An independent check of the experimental normalization was performed at the Lawrence Livermore Laboratory cyclograaff facility using an Enge split-pole spectrograph.

III. RESULTS AND DISCUSSION

A. General results and distorted-wave Born-approximation calculations

Representative data from the $^{152}\text{Eu}(d, t)$ and (d, p) runs are shown in Figs. 2 and 3. Each spectrum displayed was prepared by merging the results from two overlapping 2048-channel energy bites in the following way: The raw data from each bite were first calibrated for energy and placed on a

common intensity scale. A new spectrum was then constructed point by point by partitioning the counts according to energy and placing them into a new 2 K array. As a result, the spectra are compacted versions of the original data and have abscissas that are linear in energy.

The overall energy resolution ranged between 8–12-keV full width at half maximum (FWHM). Most of the charged-particle groups observed below ~ 1 MeV are very probably resolved singlets. Above this energy the density of levels accessible by either a (d, p) or (d, t) reaction is high enough to preclude the resolution of individual states (see Sec. III C). For this reason, we have made no attempt to assign specific structures to any of these higher-lying states. A summary of the levels populated in these studies is given in Tables I and II.

A distorted-wave Born-approximation (DWBA) analysis of the angular distribution data was performed using the code DWUCK³¹ and the optical model parameters^{32,33} shown in Table III. The deuteron-triton parameters have been successfully used by Song *et al.*³⁴ to describe results from the $^{168}\text{Er}(d, t)$ reaction at 17 MeV. A deuteron-proton parameter set similar to ours has been used successfully by Oelert *et al.*³⁵ in studies of the $^{149}\text{Sm}(d, p)$ reaction at 12.5 and 17.0 MeV. In our calculations we used nonlocality parameters

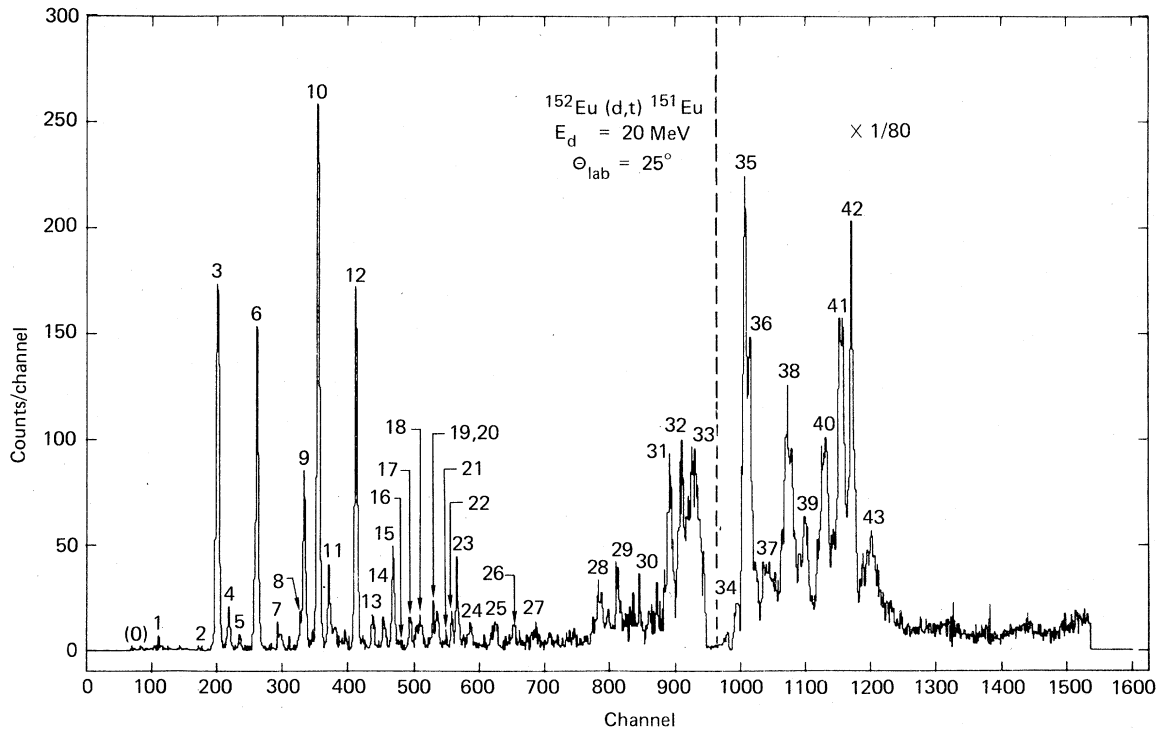


FIG. 2. Experimental spectrum: $^{152}\text{Eu}(d, t)$. The region to the right of the dashed line has been decreased by $\frac{1}{80}$. The energies of the numbered groups are given in Table I.

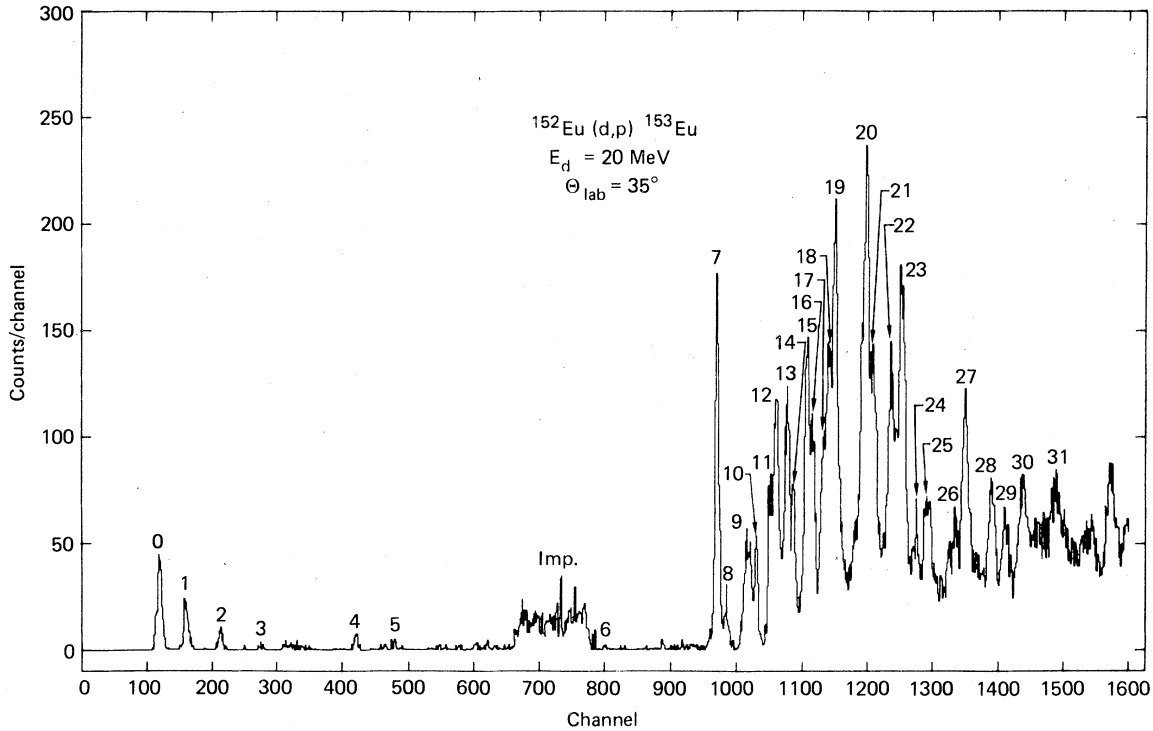


FIG. 3. Experimental spectrum: $^{152}\text{Eu}(d,p)$. The energies of the numbered groups are given in Table II.

for the charged particles: $\beta_p = 0.85$, $\beta_d = 0.54$, and $\beta_t = 0.25$. Also, finite range parameters of 0.845 and 0.621 were used for the pickup and stripping reactions, respectively.

B. Energy spectrum below 2 MeV

Inelastic scattering studies on $^{152,153}\text{Eu}$ have demonstrated^{26,27} that the ground states of these transitional nuclei have both large deformations ($\beta_2 \sim 0.3$) and very well-behaved ground state rotational structures. The ground state structures of both nuclei are also known³⁶⁻³⁸: ^{152}Eu , $\{\pi_{\frac{5}{2}}^-[413]; \nu_{\frac{1}{2}}^+[505]\}_3^-$ and ^{153}Eu , $\pi_{\frac{5}{2}}^-[413]$. The angular distributions of the (d,p) population of the $\pi_{\frac{5}{2}}^-[413]$ one-quasiparticle ground state rotational band of ^{153}Eu are shown in Fig. 4. Agreement of the experimental results with the DWBA analysis using deformed Nilsson wave functions is quite good. The data exhibit an angular distribution consistent with a pure $l=5$ signature and this virtually confirms the presence of the $\frac{1}{2}^+[505]$ neutron orbital in the two-quasiparticle ground state of ^{152}Eu .

Above the ground band, the levels observed at 616 and 733 keV, as well as the tentative level at 1400 keV together show a single-particle strength of $\sim 16\%$ of the ground band. These levels account for the remainder of the observed single-particle strength below the energy gap. A majority of this

remaining strength $\sim 9\%$ is concentrated in the 616-keV level. The level is also observed in Coulomb excitation experiments³⁹ and is therefore probably a collective vibration with a small admixture of the $\pi_{\frac{5}{2}}^-[413]$ orbital. The nature of the remaining levels at 733 and 1400 keV cannot be determined from the present experiments.

In summary, the distribution of the $^{152}\text{Eu}(d,p)$ single-particle strength below ~ 2 MeV can be understood in terms of structures that are characteristic of a strongly deformed nucleus. The spectrum virtually shows only these simple structures until one reaches an excitation energy of ~ 2 MeV. Above this energy the strength presumably results from the population of three-quasiparticle configurations where the proton and one neutron are coupled to $\{\pi_{\frac{5}{2}}^-[413], \nu_{\frac{1}{2}}^+[505]\}_{K=3}$.

By contrast to the simple situation presented by the $^{152}\text{Eu}(d,p)$ reaction, the spectrum from $^{152}\text{Eu}(d,t)$ below ~ 2 MeV shows severe fragmentation of the single-particle pickup strength. In addition, below ~ 2 MeV, as noted in Table I, there is almost complete correspondence between the levels populated in (d,t) and (p,t) , although there are small relative differences in the degree of populating specific states. As noted previously, Dracoulis and Leigh²³ have suggested a description of the low-lying positive structures in ^{151}Eu

TABLE I. Nuclear levels in ^{151}Eu . A comparison of the levels populated in the (d, t) and (p, t) reactions are given in columns 2 and 3. Spin-parity assignments and adopted levels from Ref. 11 are noted in columns 4 and 5. Level energies in column 1 enclosed in parentheses indicate that there is only weak evidence that the level is populated. An asterisk (*) indicates a probable multiplet. The uncertainties noted are purely statistical.

(d, t) group	Level energy		I	Adopted (keV)	(d, t) group	Level energy		I	Adopted (keV)
	(d, t) (keV)	(p, t) (keV)				(d, t) (keV)	(p, t) (keV)		
0	(0)	(0)	$\frac{5}{2}^+$	0	22	1178 ± 3	1176		1154
1	22 ± 6	22	$\frac{7}{2}^+$	21.54	23	1200 ± 3	1200		1200
2	196 ± 6		$\frac{11}{2}^-$	196.21	24	1252 ± 3	1247		1247
3	260 ± 1	261	$\frac{5}{2}^+$	260.44	25	1346 ± 4	1338		1338
4	306 ± 2	309	$\frac{5}{2}^+$	307.47	26	1420 ± 3			1425
5	350 ± 2		$\frac{3}{2}^-$	349.76	27	1506 ± 3			(1497)
6	415 ± 1	414	$(\frac{7}{2}^+)$	415.0	28	1762 ± 4			
7	505 ± 2	508	$\frac{3}{2}^+$	503.5	29	1833 ± 4			
8	584 ± 2	585	$(\frac{5}{2}^+)$	581.0	30	1912 ± 4			
9	600 ± 1	597	$(\frac{3}{2}^+)$	601.0	31	2022 ± 3			
10	654 ± 1	654	$(\frac{5}{2}^+)$	654.0	32	2072 ± 3			
11	697 ± 1	698	$(\frac{5}{2}^+)$	698.0	33	$2110 (*)$			
12	802 ± 1	801		801.0	34	2307 ± 5			
13	868 ± 2	869		869.0	35	2331 ± 4			
14	910 ± 2	911		911.0	36	2348 ± 4			
15	947 ± 2	944		944.0	37	2419 ± 6			
16	(972)				38	2494 ± 4			
17	1014 ± 3			1016.0	39	2510 ± 5			
18	$1049 (*)$			(1036.0)	40	2644 ± 4			
19	1102 ± 3	1097		1092	41	2711 ± 4			
20	1120 ± 3	1117		1117	42	2751 ± 4			
21	1151 ± 3	1154		1154	43	2827 ± 6			

in terms of mixtures of weakly deformed Nilsson states. They also point out that this description is consistent with the (p, t) results. We now wish to consider this weakly deformed picture in light of the experimental data from the (d, t) reaction. The comparison can be made fairly quantitatively because the ^{152}Eu target state has a simple two-quasiparticle structure and is well characterized. Also, the analysis of the (d, p) results suggests confidence in the DWBA calculations. A similar analysis of the (p, t) reaction is far less straightforward. For example, although (p, t) $l=0$ transfer gives an unambiguous signature, for other l transfer values the angular distributions tend to have no pronounced structure and are sensitive to details of the structure of the initial and final states as well as to higher-order multistep processes.⁷ For $^{153}\text{Eu}(p, t)$ in particular, more complexities arise from possible l admixtures due to

the nonzero spin of the target.

In Figs. 5 and 6 we present a comparison of the experimental and calculated differential cross sections for the proposed deformed band in ^{151}Eu at 260 keV. The cross sections were calculated assuming that the final state configuration is $\pi \frac{5}{2} [413]$ and the calculated results were reduced by a factor of 3.2 to align them with the experimental data. Figure 5 shows that the experimental angular distributions for the band members are consistent with a pure $l=5$ signature, and Fig. 6 is a comparison of the calculated and experimental intensities near the maximum of the $l=5$ distribution. Except for the $\frac{11}{2}^+$ state, the angular distributions of the lower-lying levels, as well as their predicted relative intensity pattern, are in excellent agreement with the data and are certainly suggestive of the assigned rotational character for these states. The fact that the full strength

TABLE II. Levels in ^{153}Eu populated in the ^{152}Eu (d, p) reaction. Level energies enclosed in parentheses indicate that there is only weak evidence that the level is populated. An asterisk (*) indicates a probable multiplet. The uncertainties noted are purely statistical.

(d, p) group	Level energy (keV)	(d, p) group	Level energy (keV)
0	0 ± 1	16	2045 ± 3
1	83 ± 1	17	2082 ± 5
2	191 ± 2	18	2099 ± 4
3	319 ± 4	19	2118 ± 3
4	616 ± 2	20	2218 ± 3
5	733 ± 3	21	2236 ± 5
6	(1400)	22	2294 ± 4
7	1748 ± 3	23	2327 ± 4
8	1777 ± 4	24	2368 ± 6
9	1843 (*)	25	2408 (*)
10	1870 ± 4	26	2496 ± 5
11	1915 ± 4	27	2527 ± 4
12	1932 ± 3	28	2610 ± 4
13	1961 ± 3	29	2651 ± 5
14	1982 ± 3	30	2707 ± 5
15	2028 ± 3	31	2808 (*)

(d, t) intensity appears hindered by a factor 3–4 can be understood in terms of differences in the deformations of the target and residual states.

If the position of the $\frac{11}{2}^+$ state is, in fact, 845.3 keV as suggested by Taketani *et al.*,¹⁹ the failure of the (d, t) reaction to populate the state is disturbing. Our DWBA calculations suggest that the state should be observed at 25° and 35°, where the predicted intensity is well above the experimental detection limit, and the spectral region is relatively free of interfering particle groups. However, the results of Taketani *et al.* on the nature of the 845-keV state are not entirely unambiguous. In particular, whereas the observed cascade to crossover decay ratio for the $\frac{9}{2}^+ \rightarrow \frac{7}{2}^+ \rightarrow \frac{5}{2}^+$ states agrees reasonably well with the corresponding ratio in ^{153}Eu , the ratio for the $\frac{11}{2}^+ \rightarrow \frac{9}{2}^+ \rightarrow \frac{7}{2}^+$ decay is a factor of 4–16 higher than that measured in ^{153}Eu . In spite of the obvious discrepancies noted for the 845.3-keV state, the weight of evidence from in-beam and charged-

particle work for a rotational interpretation of the 260-, 415-, and 600-keV states is difficult to ignore.

The ground and 22-keV states in ^{151}Eu have spin parities of $\frac{5}{2}^+$ and $\frac{7}{2}^+$, respectively. Population of the ground state is not observed in our (d, t) studies and the 22-keV state is only weakly populated. At a scattering angle of 25° the 22-keV state has a measured cross section of $0.5 \pm 0.1 \mu\text{b/sr}$ and the upper limit on population of the ground state is $< 0.09 \mu\text{b/sr}$. Dracoulis and Leigh²³ have suggested that the levels near the ground state are weakly deformed ($\beta_2 \sim 0.11$) and that the ground state is the $\frac{5}{2}^+$ member of a band built on the $\pi \frac{3}{2}^+$ [411] Nilsson orbital while the 22-keV state is primarily the $\frac{7}{2}^+$ member of a $\pi \frac{7}{2}^+$ [404] band. The $\frac{5}{2}^+$ [413] band at 260 keV was also considered weakly deformed but with a deformation $\sim 45\%$ larger (0.16) than the other lower-lying states and a factor of ~ 2 smaller than the measured deformation^{26,27} (~ 0.28) of the ^{152}Eu ground state. The authors then performed a Coriolis-mixing calculation which reproduced reasonably well the low-lying level sequence of ^{151}Eu . The wave functions derived from this calculation show that the ground state had a small ($\sim 2\%$) component of the $\frac{5}{2}^+$ [413] orbital and that a much larger component ($\sim 30\%$) of this orbital is present in the 22-keV state. If we combine these admixtures with our predicted cross sections for a pure $\frac{5}{2}^+$ [413] configuration at 25°, we predict $2 \mu\text{b/sr}$ and $21 \mu\text{b/sr}$ for the 0- and 22-keV states, respectively. Combining the calculated cross sections with our experimental results, we estimate hindrance factors of > 22 and 42 ± 8 , respectively, for population of these states with the (d, t) reaction. Recalling that the (d, t) hindrance from a target with $\beta_2 = 0.28$ to the 260-keV band ($\beta_2 = 0.16$) is only 3–4, it would seem that the nature of at least the 0- and 22-keV states ($\beta_2 = 0.11$) significantly differs from that proposed by Dracoulis and Leigh. This analysis in conjunction with the other measured properties^{12–15} of these states strongly argues for their interpretation as nearly spherical structures.

The strongly excited states at 654 and 801 keV have been discussed in detail by Taketani *et al.*,⁷

TABLE III. Optical model parameters.

	V_r (MeV)	r_r (fm)	r_c (fm)	a_r (fm)	W (MeV)	W_D (MeV)	r_I (fm)	a_I (fm)	V_{so} (MeV)	r_{so} (fm)	a_{so} (fm)	λ_{so}	Ref.
$^{152}\text{Eu} + d$	100.2	1.15	1.15	0.81		19.2	1.34	0.68					32
$^{151}\text{Eu} + t$	166.7	1.16	1.40	0.75	16.4		1.50	0.82					33
$^{153}\text{Eu} + p$	54.5	1.17	1.25	0.75	3.1	7.3	1.32	0.51	6.2	1.01	0.75		32
Bound state	a	1.25	1.25	0.65								25.0	

^a Adjusted to give the correct separation energy: for (d, p), $S(n) = 2.22 + Q(d, p)$; for (d, t), $S(n) = 6.26 - Q(d, t)$.

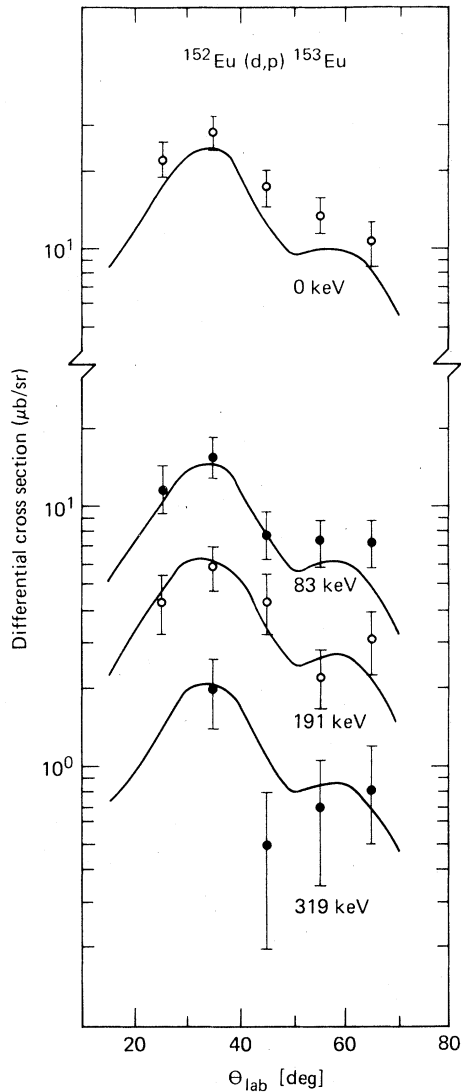


FIG. 4. Angular distributions for the (d,p) excitation of the ^{153}Eu ground state rotational band. The solid lines are the theoretical angular distributions evaluated from the relation

$$\sigma(\theta) = 1.5 \cdot \langle I_i j - K_i \Omega | I_f K_f \rangle^2 \cdot C_{j_i}^2 \cdot U^2 \cdot \Phi_{j_i}(\theta)$$

using $U^2 = 0.5$. Each level exhibits a pure $l=5$ angular distribution because the $\frac{1}{2}^+$ [505] neutron component of the target state has only the $h\frac{1}{2}^+$ spherical component.

and have been assigned as the $\frac{5}{2}^+$ and $\frac{7}{2}^+$ members of a collective β vibration built on the 260-keV deformed band. In the (d,t) reaction these levels are populated somewhat more strongly ($\sim 10\%$) than the members of the lower-lying deformed band. In Fig. 7 we present a comparison of the experimental and calculated (d,t) differential cross sections for the band beginning at 654 keV. The cross sections were calculated assuming that the final-state configuration is pure $\pi\frac{5}{2}^+$ [413] and were

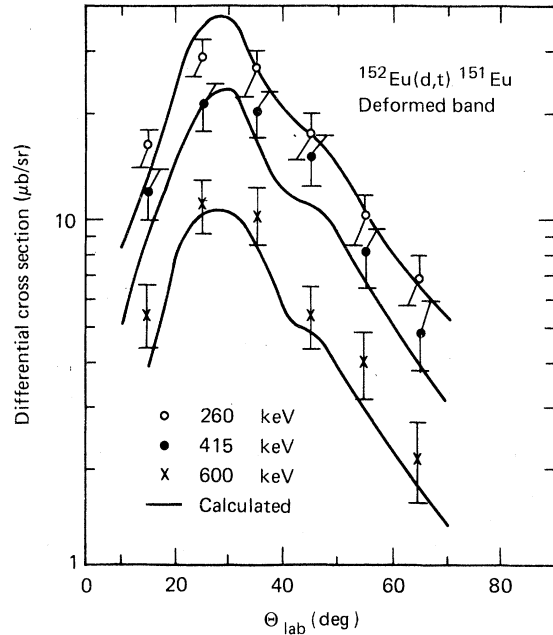


FIG. 5. Angular distributions for (d,t) excitation of the $\frac{5}{2}^+$, 260-keV deformed band in ^{151}Eu . The solid lines are the theoretical angular distributions for a pure $\pi\frac{5}{2}^+$ [413] deformed residual state but reduced by a factor 3.2.

reduced by a factor of 3 to align the experimental and calculated values for the 654- and 802-keV states. To the extent that it is possible to understand the observed intensity pattern in this simple way, we predict that the $\frac{3}{2}^+$ and $\frac{1}{2}^+$ members of the band have observable cross sections. Of the levels excited in the (d,t) and (p,t) reactions, the (d,t) intensities of the levels at 947 and 1102 keV most closely correspond to the values predicted

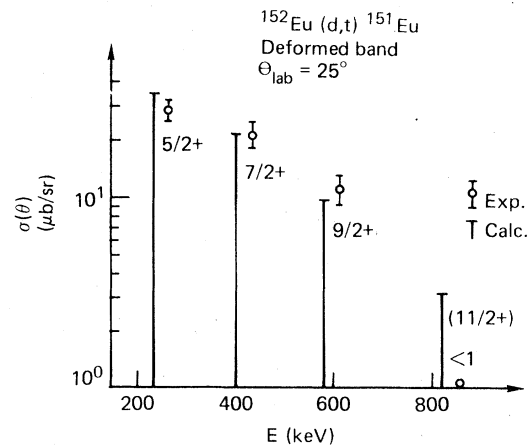


FIG. 6. Comparison of the experimental and calculated (d,t) intensity patterns for the $\frac{5}{2}^+$, 260-keV deformed band in ^{151}Eu . See Fig. 5.

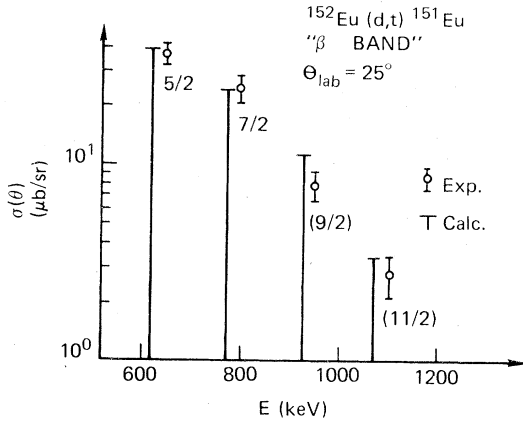


FIG. 7. Comparison of the experimental and calculated (d, t) intensity patterns for the $\frac{5}{2}^+$, 654-keV deformed band in ^{151}Eu . The calculated cross sections are the values for a pure $\pi\frac{5}{2}^+$ [413] residual state reduced by a factor 3.

and we tentatively assign them as $\frac{9}{2}^+$ and $\frac{11}{2}^+$ members of the band. Although the assignment of these states as additional rotational levels seems reasonable on the basis of the cross-section data, it is somewhat questionable for two reasons. First, recalling that the (d, t) reaction apparently does not excite the $\frac{11}{2}^+$ state of the 260-keV band near the predicted intensity, it is not clear what level of confidence should be placed in such simple comparisons. If a simple mechanism (e.g., Coriolis effects) could account for this obvious discrepancy, the cross-section comparisons noted for both bands would be made significantly more sound. A second difficulty becomes apparent when one compares the rotational parameters derived from the energy differences in both bands. Going up the levels in each band ($\frac{5}{2}^+$ to $\frac{11}{2}^+$), the derived sequence of $\hbar^2/2\mathcal{J}$ values¹⁹ is 22.2, 20.5, and 22.3 keV for the 260-keV band and 21, 16, and 14 keV for the 654-keV band. The apparent strong compression of the rotational parameters for the higher-energy band relative to an almost constant value for the lower-lying band suggests either strong rotational particle coupling or a strong centrifugal stretching effect. In either case, it is not clear what level of validity could then be made in simple cross-section comparisons that do not take account of these factors. On the other band, if the 845.3-keV state observed by Taketani *et al.* is not the $\frac{11}{2}^+$ member of the 260-keV deformed band, and the rotational level actually has a lower energy which is consistent with a downward trend in $\hbar^2/2\mathcal{J}$, then the spin-dependent trend of the rotational parameters for the 654-keV band would suggest a comparatively less perturbed situation. Furthermore, a lower value of $\hbar^2/2\mathcal{J} \sim 18$ keV for the $\frac{9}{2}^+ - \frac{11}{2}^+$ separation in the 260-keV band (which

is consistent with the spin-dependent downward trend for this band) would place the $\frac{11}{2}^+$ state at an energy of ~ 800 keV. The predicted weak (but observable) (d, t) population of this state would then be obscured by the intense group at 802 keV.

The levels assigned to the two rotational bands in ^{151}Eu account for $\sim 60\%$ of the total $l=5$ (d, t) strength that should be observed. If we sum the intensity of the remaining weakly populated structures between 0 and ~ 1.5 MeV, then the balance of the missing strength ($\sim 40\%$) is totally accounted for. Specific assignments for these weakly populated states have not been attempted.

Summarizing our observations of the lower-energy portion of the $^{152}\text{Eu}(d, t)$ spectrum, it is at first obvious that the single-particle transfer strength obtained from a strongly deformed target shows severe fragmentation below ~ 2 MeV. Although $\sim 40\%$ of the experimental intensity is distributed almost evenly among many states (~ 20) between 0 and ~ 1.5 MeV, the majority of strength is concentrated in two groups of levels that are interpreted reasonably well as $K^\pi = \frac{5}{2}^+$ rotational bands. Also, the odd-proton quasiparticle component of each band has a reasonably good overlap ($\sim 30\%$) with a deformed ($\beta_2 = 0.28$) $\pi\frac{5}{2}^+$ [413] orbital. Second, because of the comparatively large rotational parameters ($\hbar^2/2\mathcal{J} \sim 20$ keV) derived for both bands and because they are populated with only $\sim 30\%$ of the predicted strength of a pure $\pi\frac{5}{2}^+$ [413] configuration, it is very reasonable to regard the static deformation of the $N=88$ core for these states to be *less* than that of the corresponding ground state even- N cores in either ^{152}Eu or ^{153}Eu . Both the latter have been shown²⁷ to have $\beta_2 \sim 0.28$. Finally, detailed considerations of our data appear to support a predominantly spherical structure for the ground and near-lying positive parity states in ^{151}Eu .

Although our data suggest that the core associated with each of the two strongly populated bands in ^{151}Eu is deformed, specific details concerning other aspects of the underlying nuclear structure are very uncertain. Unlike the ground state which is very probably predominantly $\pi d_{5/2}$, the two bands have an intensity pattern consistent with removing a neutron from the configuration $\{\pi\frac{5}{2}^+$ [413], $\nu\frac{11}{2}^+$ [505] $\}_{K=3^-}$ with the exception that each has only $\sim 30\%$ of the theoretical intensity. The (d, t) spectroscopic factor connecting two deformed nuclei is defined as the probability that the final state is the target ground state with the removal of a neutron having a particular (l, j) value. For the ^{152}Eu target, the neutron will be removed with only $l=5$, and the intensity ratios within any band in ^{151}Eu will resemble the theoretical values if the overlap integral of both the core and the odd-proton

wave functions do not change with angular momentum. Based on the measured (d, t) hindrances, this condition of good overlap is reasonably valid ($\sim 30\%$) for the bands starting at 260 and 654 keV. It is also interesting that both bands exhibit approximately the same hindrance. One possible model for these structures is to assume that the lower band (260 keV) results from the $\frac{5}{2} [413]$ proton coupled to a weakly deformed core. The higher band might then be a β vibration⁷ built on this configuration. Strong population of the β vibration in the (d, t) reaction can be understood because the target core is not necessarily orthogonal to states associated with the β vibration in the case where the cores of the target and residual nucleus are different. However, the higher band need not be a β vibration. The band might be based on some other 0^+ core vibration or, equally plausible, could be a "ground" rotational structure built on a somewhat more strongly deformed but relatively stable prolate core.

C. Energy spectrum above 2 MeV

The most striking feature of the $^{152}\text{Eu}(d, t)$ spectrum is the extremely strong population of states in a narrow band of excitation energies between approximately 2.3 and 2.8 MeV. Virtually all the observed pickup strength ($\sim 98\%$) is concentrated in these levels. It is our hypothesis that these states are strongly deformed ($\beta_2 \sim 0.3$) and are essentially one-neutron holes coupled to the $\{\pi \frac{5}{2} [413], \nu \frac{11}{2} [505]\}_{K=3}$ configuration, which is the ground state of ^{152}Eu . The strongest support for this hypothesis would be the identification of individual rotational bands in this energy region. Unfortunately, the presence of a high density of states and the insufficient resolution of our experiments have made this virtually impossible. As a result, we have been able to look only at the gross properties of the spectrum for an interpretation in terms of strongly deformed states. Our intent for the remainder of this section is to assume a deformed interpretation, compute the (d, t) spectrum, and compare the calculated results with the experimentally observed spectrum. A similar comparison will also be made for the (d, p) spectrum.

An immediate difficulty in reproducing the gross spectral properties of deformed levels with $E_{\text{ex}} > 2$ MeV is the uncertain knowledge of the energy distribution of these states. Although this can be calculated in a deformed model, we have instead chosen a semiempirical approach since it is not clear that our conclusions would differ significantly if based on a more rigorous approach.

In Table IV we present a list of Nilsson single-

TABLE IV. Estimated zero-point energies for deformed three-quasiparticle^a states in $^{151,153}\text{Eu}$.

Active neutron $\Omega(Nn_z \Lambda)$	E_0^b (keV)	V^2^c
$\frac{7}{2} [404]$	3495	0.94
$\frac{9}{2} [514]$	3117	0.92
$\frac{1}{2} [530]$	2623	0.85
$\frac{1}{2} [400]$	2567	0.83
$\frac{3}{2} [402]$	2467	0.80
$\frac{3}{2} [532]$	2460	0.79
$\frac{11}{2} [505]$	2319	0.72
$\frac{1}{2} [660]$	2265	0.67
$\frac{3}{2} [651]$	2223	0.63
$\frac{3}{2} [521]$	2200	0.50
$\frac{5}{2} [642]$	2405	0.23
$\frac{5}{2} [523]$	2522	0.18
$\frac{1}{2} [521]$	2756	0.13
$\frac{5}{2} [512]$	3150	0.08
$\frac{7}{2} [633]$	3200	0.07

^a The active neutron is assumed to be coupled to $\{\pi \frac{5}{2} [413]; \nu \frac{11}{2} [505]\}_{K=3}$.

^b Calculated assuming $\Delta = 1.1$ MeV. E_0 represents the center of gravity energy of the parallel and antiparallel couplings of the active neutron to the $K=3$ two-quasiparticle ground state of ^{152}Eu . For ^{151}Eu , E_0 is increased by 260 keV because the "deformed ground state" has an excitation energy of 260 keV.

^c V^2 are the occupation probabilities of the active neutrons in the ^{152}Eu target and are required to compute the (d, t) cross sections. For the (d, p) cross section calculations, we use $V^2 = 1 - V^2$.

particle states used in our calculations. For the most part the orbitals are chosen on the basis of experimental observations of states below ~ 1 MeV by Tj m and Elbek⁴⁰ in (d, p) and (d, t) studies of the deformed $N = 91$ nucleus ^{155}Gd . Since Nilsson model calculations suggest that other states are distributed among those observed in the stripping and pickup studies of ^{155}Gd , we have also included some of these in our tabulation. Those predicted "missing" states that would show strong population in (d, p) or (d, t) (i.e., $\frac{5}{2} [402]$) have not been included because they would have been observed if they contributed to structures below ~ 1 MeV. The remainder of the predicted states, which would be only weakly populated in stripping and pickup experiments, are included in our tabulation. This latter group of states is somewhat important because it forms part of the continuum on which the more strongly populated states rest. Generally,

these weakly excited states would not be expected to markedly alter any strong detail present in the stripping or pickup spectrum, and consequently their energy uncertainty can be virtually ignored. We require only that some measure of their effect be included in the rather wide energy range (~ 1 MeV) we are considering. The single-particle energies of these "missing" states have been calculated⁴¹ in the Nilsson model¹⁸ using $\beta_2=0.28$, $\beta_4=0.05$, $\mu=0.48$, and $\kappa=0.05$. The quasiparticle energies of both the calculated and experimentally observed neutron states are estimated relative to the $\frac{3}{2}^- [521]$ orbital. Pairing factors relating to the neutron orbitals in the ^{152}Eu target are derived from the one-quasiparticle energies and the energies of the three-quasiparticle residual states are calculated from the one-quasiparticle energies, and using⁴² $\Delta=1.1$ MeV. The single-particle wave functions for all states have been taken from the Nilsson model calculation previously described. By using the deformed neutron states associated with the $N=90$ ^{155}Gd core, we are implicitly assuming that within an interval of ~ 1 MeV the same states are also the main components of the deformed three-quasiparticle states coupled to what is now an $N=86$ ^{151}Eu core. If the $N=86$ core associated with these states is in fact deformed, then

this is a reasonable approximation. We do not expect, however, anything approaching detailed correspondence of the single-particle energies between either core.

The coupling of the odd-neutron quasiparticle to the two-quasiparticle configuration which represents the ^{152}Eu ground state will split the single-particle strength into two bands separated generally by several tens of keV. To present a more realistic distribution of this splitting, we have used calculated splittings³⁷ from the odd-odd nucleus ^{152}Eu which involve the $\frac{5}{2}^+ [413]$ proton orbital and various neutron configurations. For orbitals not considered in Ref. 37, we have arbitrarily assumed a splitting of 100 keV. The bands built on each configuration were assumed to have a constant value $\hbar^2/2\mathcal{J}=12$ keV. Based on these assumptions, we have calculated the spectroscopic factors for each state of the various bands and used these along with the DWBA results to obtain predicted (d,t) and (d,p) cross sections. To partially account for configuration mixing, we distributed the cross section symmetrically about the calculated position of each state using an energy-dependent Lorentz⁴³ factor. The experimentally observed and calculated (d,t) and (d,p) spectra are presented for comparison in Fig. 8. The experimental

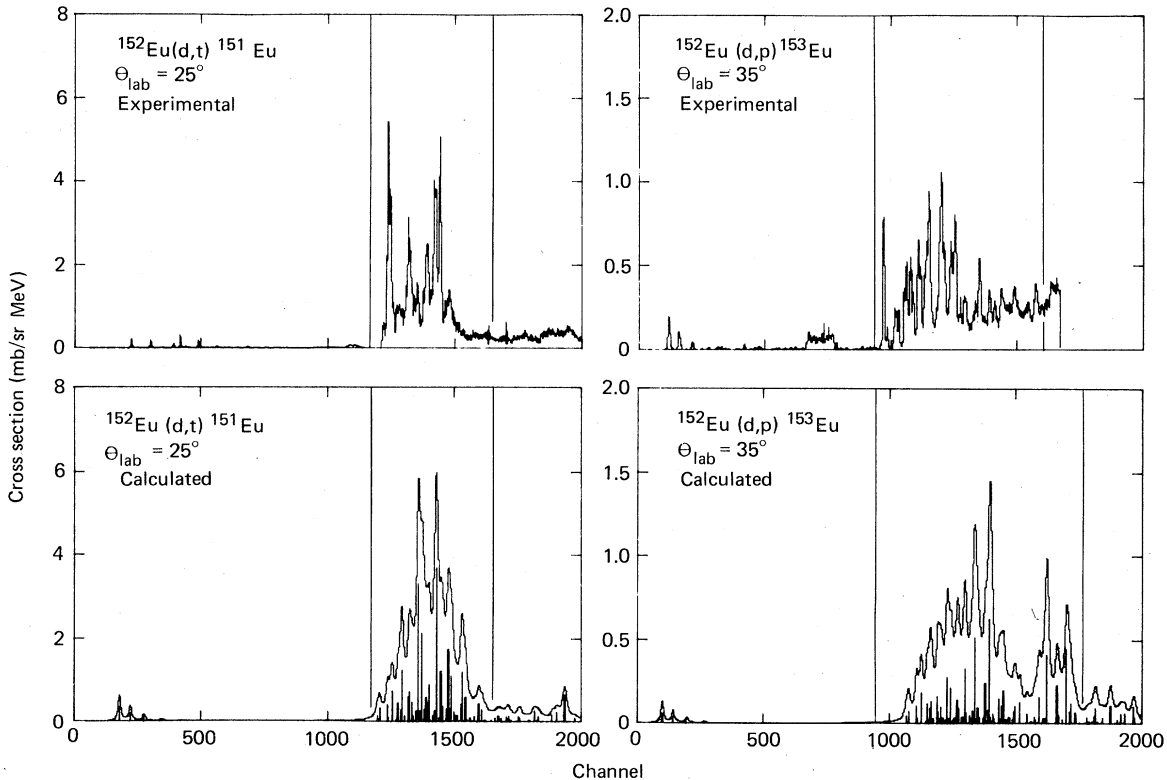


FIG. 8. Comparison of the experimental and calculated (d,t) and (d,p) spectra from a ^{152}Eu target. The angular distributions of the total intensity contained in each window are compared in Fig. 9. See text.

angular distributions of the integrated strength for the states between 2.1 and 3.2 MeV for (d, t) and 1.7 and 2.9 MeV for (d, p) are compared with the calculated results at the top of Fig. 9.

In Fig. 8 the calculated spectral distribution⁴⁴ for the $^{152}\text{Eu}(d, t)$ reaction for $E_{\text{ex}} > 2$ MeV shows very clearly that there is agreement with the general features of the experimental data. In particular, both the spectral intensity and its concentration in a rather narrow energy range can be accounted for. Although the individual and particular features of this region are not reproduced exactly, it is interesting to note that a count of the discrete peaks above any arbitrary intensity cut-off (say, 20% of the maximum intensity displayed by the strongest group) usually agrees with the experimental observations. In the $^{152}\text{Eu}(d, p)$ reaction, one is confident that the states excited above ~ 2 MeV are, in fact, deformed. Comparing the experimental and calculated (d, p) spectra (Fig. 8) shows that our crude calculation again agrees reasonably well with experiment. In the calculated (d, p) spectrum, the strong pair of peaks that appear at ~ 3 MeV are due to the $\frac{1}{2}[521]$ orbital. The experimental data on the Gd nuclei show that this orbital becomes lower in energy relative to the $\frac{3}{2}[521]$ orbital for progressively larger mass numbers. For the three-quasiparticle states in ^{153}Eu , if we had chosen single-particle states from ^{157}Gd instead of ^{155}Gd , the net effect would have

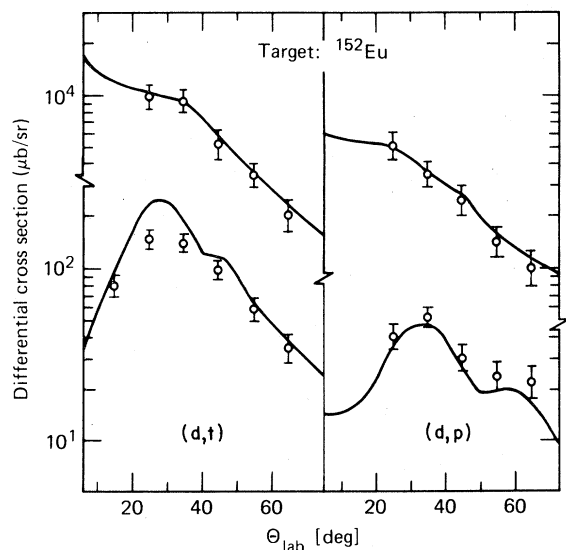


FIG. 9. Integrated experimental and theoretical angular distributions from the (d, t) and (d, p) reactions. The upper half of the figure compares the data and calculated results in the vertical window noted in Fig. 8. The lower half compares similar integrated results for the two deformed bands in ^{151}Eu and for the ground state band of ^{153}Eu . See text.

been to move the levels from the $\frac{1}{2}[521]$ orbital more closely toward the high-density region of the spectrum and thereby improve the agreement with the experimental (d, p) profile.

A comparison of the total spectral profile (0 to ~ 3 MeV) for both reactions shows an interesting contrast. The experimental (d, p) spectrum over the whole energy range looks much like the calculated profile. The experimental (d, t) spectrum, however, shows general agreement with $E_{\text{ex}} > 2$ MeV but is severely fragmented in the low-energy (< 1.5 MeV) region.

The angular distributions noted in Fig. 9 present more detail on the gross spectral properties observed in both reactions. The upper half of Fig. 9 compares experimental and calculated angular distributions of integrated cross sections for the high-energy region. The windows in which the intensity summation was carried out for each angle are noted in Fig. 8. It is clear that the experimental data follow rather well the curves obtained from our calculations which assume deformed final states. The lower half of Fig. 9 compares the cross section integrated angular distributions of the low-lying deformed states. The experimental and calculated shapes agree reasonably well. In the (d, t) reaction, although the experimental and calculated shapes are similar, the calculated curve is somewhat higher than the experimental data. This discrepancy occurs because the measured intensities of only the 260- and 654-keV bands have been used to generate the experimental data points. The solid curve is the calculated total intensity assuming a deformed final state. The remaining intensity not measured in these bands can be accounted for and is spread out over a number of nearby states. A similar comparison of the (d, p) data shows that the ground state band contains virtually all the predicted $l=5$ strength.

The experimental data and its comparison with our crude calculations suggest that the structures with $E_{\text{ex}} > 2$ MeV observed in ^{151}Eu can be reasonably interpreted as deformed three-quasiparticle states coupled to a core that has a deformation as large as the ^{152}Eu ground state. The presence of strongly deformed individual structures in ^{151}Eu would be interesting to isolate. Unfortunately our experimental resolution was not adequate to separate cleanly any individual peaks above 2 MeV. The line structures noted in the lower half of Fig. 8 represent the theoretical spectra prior to Lorentzian spreading. It is clear that there exists a large number of closely packed states that would be difficult to resolve. However, a few have large intensities, and some idea of individual characteristics may be obtained.

The best resolved structure in the ^{151}Eu spec-

trum is the obvious doublet (peaks 35 and 36 in Fig. 2) at ~ 2340 keV (2331 ± 4 and 2348 ± 4 keV). Our calculations (Fig. 8) suggest that the group is composed primarily of three-quasiparticle band heads involving $3^- \otimes \frac{1}{2} [400]$ and $3^- \otimes \frac{3}{2} [402]$. Since we have not performed calculations that would suggest which resultant spins are lowest, four possible spin combinations, which could give rise to the doublet group, are equally valid. Therefore, one may have the combinations $(\frac{5}{2}, \frac{9}{2})$, $(\frac{5}{2}, \frac{3}{2})$, $(\frac{7}{2}, \frac{9}{2})$, and $(\frac{7}{2}, \frac{3}{2})$ for 3^- coupling with the $\frac{1}{2} [400]$ and $\frac{3}{2} [402]$ orbitals, respectively. In Fig. 10 we have plotted the experimental angular distribution of the doublet group along with the calculated angular distributions of each pair of spin combinations. From the comparison one sees various levels of agreement, but the calculated shapes are all in general agreement with the data. More importantly, however, the states ap-

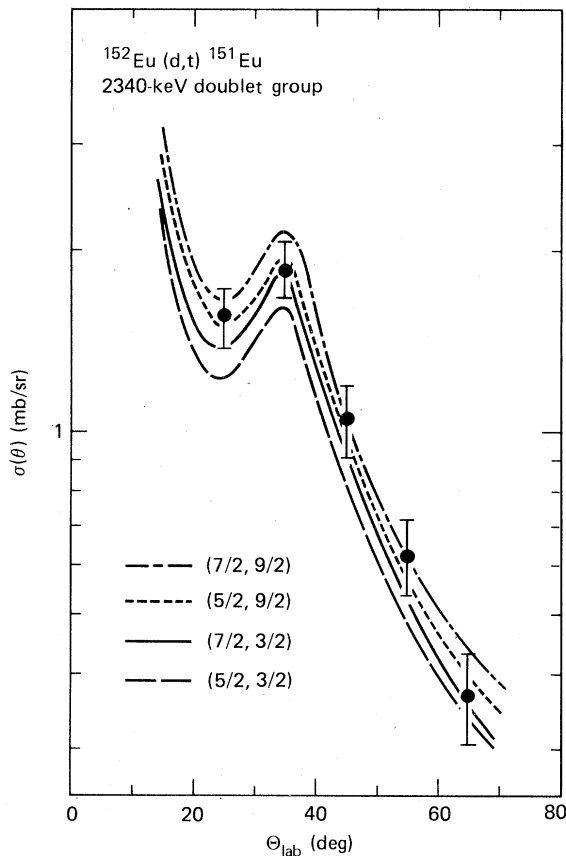


FIG. 10. Angular distribution of the ~ 2340 -keV (group nos. 35 and 36, Fig. 2) triton group from the $^{152}\text{Eu}(d,t)^{151}\text{Eu}$ reaction. The group is assumed to be composed of two closely spaced band heads involving the three-quasiparticle components: $\{3^- \otimes \frac{3}{2} [402]\}$ and $\{3^- \otimes \frac{1}{2} [400]\}$. As noted, each curve is the calculated angular distribution for an alternate pair of valid spin assignments for the assumed components. See text.

pear experimentally to possess (whichever assignment one chooses) virtually the full intensity as predicted for deformed states and do not exhibit the large degree of fragmentation that is so evident with the lower-lying levels. This analysis, however, does not consider a possible near degeneracy of the two different band heads derived from the same three-quasiparticle coupling. The angular distributions calculated for these possibilities are, on average, $\sim 32\%$ higher $\{3^- \otimes \frac{1}{2} [400], K = \frac{5}{2}, \frac{7}{2}\}$ and $\sim 38\%$ lower $\{3^- \otimes \frac{3}{2} [402], K = \frac{3}{2}, \frac{9}{2}\}$ than the experimental data. Although this would appear to experimentally rule out such a degeneracy, it is clearly not a totally unambiguous result because the data do not involve well-isolated peaks and the errors may be large.

In summary, although our considerations of the gross properties of the high-energy (d,t) spectrum, in general, and of the ~ 2340 -keV triton doublet group, in particular, cannot be regarded as totally convincing proof that strongly deformed structures exist in ^{151}Eu above ~ 2 MeV, they are at least highly suggestive. On this basis it would be interesting to further test this hypothesis with more quantitative calculations and higher resolution experiments.

IV. CONCLUSIONS

The role played by blocking of the steeply up-sloping $\frac{11}{2} [505]$ orbital in determining the degree of prolate deformation of odd-neutron transitional nuclei has been discussed in detail by Kleinheinz *et al.*⁹ Our studies appear to support their conclusions. The ground state of the ^{152}Eu target used in our experiments contains the $\frac{11}{2} [505]$ neutron as one of its two quasiparticle components. Excited states which essentially maintain intact this ^{152}Eu ground state coupling determine unambiguously a 50% occupation probability for the $\frac{11}{2} [505]$ orbital. A number of such three-quasiparticle states are, of course, populated in single nucleon pickup and stripping. The only one-quasiparticle states that one expects to be strongly populated by single-neutron transfer involve emptying or filling the $\frac{11}{2} [505]$ orbital. For these one-quasiparticle states in ^{151}Eu , the final state occupation probability of the $\frac{11}{2} [505]$ orbital is very likely $> 50\%$ because the orbital lies significantly below the Fermi surface for most reasonable deformations with $N < 90$.

On this basis we can interpret the (d,t) spectrum in the following way. First, the ^{151}Eu ground state is essentially spherical, but the nuclear potential is very soft toward β deformation. Populating these states is virtually forbidden by the (d,t) reaction. A small increase in excitation energy presumably takes the nucleus to a second minimum

where it has a small but relatively stable prolate deformation. The 260-keV rotational band forms the "ground band" of this potential. The hindered (d, t) population as well as a high value for the rotational parameter is evidence that the core is only weakly deformed. We can further speculate that the $\frac{11}{2} [505]$ neutron orbital in this potential is essentially filled and thus offers resistance toward full deformation of the core. Finally, three-quasiparticle states which involve one neutron confined to the $\frac{11}{2} [505]$ orbital fix the occupation probability at 50% and the associated states can be strongly deformed. The states in this "third minimum" are strongly populated, appear unfragmented, and are therefore probably virtually pure deformed states.

When two more neutrons are added to form $^{153}\text{Eu}(N=90)$, the Fermi surface shifts upwards, and the upsloping effect of the $\frac{11}{2} [505]$ orbital is essentially offset by increased pair scattering into

available downsloping orbitals. Even though ^{153}Eu has a fairly large ground state deformation, it may be that the degree of occupation of the $\frac{11}{2} [505]$ orbital still has a significant effect on the deformation. If this is true, then higher-energy three-quasiparticle states involving the unpaired (blocked) $\frac{11}{2} [505]$ orbital ($U^2, V^2=0.5$) may be more strongly deformed than one-quasiparticle structures near the ground state where the orbital is not blocked. Somewhat more precise experiments than those reported here would be necessary to test this hypothesis.

ACKNOWLEDGMENTS

We wish to thank the staffs of the accelerator facilities at the Los Alamos Scientific Laboratory and at the Lawrence Livermore Laboratory under Contract No. W-7405-Eng-48.

*Present address: Department of Physics, The Technical University of Munich, Garching, Germany.

¹J. H. Bjerregaard, O. Hansen, and O. Nathan, Nucl. Phys. **86**, 145 (1966).

²J. R. Maxwell, G. M. Reynolds, and N. M. Hintz, Phys. Rev. **151**, 1000 (1966).

³R. Chapman, W. McLatchie, and J. E. Kitching, Nucl. Phys. **A186**, 603 (1972).

⁴P. Debenham and N. M. Hintz, Phys. Rev. Lett. **25**, 44 (1970).

⁵D. G. Fleming, C. Günther, G. B. Hagemann, and B. Herskind, Phys. Rev. Lett. **27**, 1235 (1971).

⁶D. G. Burke, G. Løvholden, and J. C. Waddington, Phys. Lett. **43B**, 470 (1973).

⁷H. Taketani, H. L. Sharma, and N. M. Hintz, Phys. Rev. C **12**, 108 (1975).

⁸D. G. Burke, E. R. Flynn, J. D. Sherman, and J. W. Sunier, Nucl. Phys. **A258**, 118 (1976).

⁹P. Kleinheinz, R. K. Sheline, M. R. Maier, R. M. Diamond, and F. Stephens, Phys. Rev. Lett. **32**, 68 (1974).

¹⁰W. B. Cook, M. W. Johns, G. Løvholden, and J. C. Waddington, Nucl. Phys. **A259**, 461 (1976).

¹¹B. Harmatz, Nucl. Data Sheets **19**, 33 (1976).

¹²J. E. Thun and T. R. Miller, Nucl. Phys. **A193**, 337 (1972).

¹³E. M. Bernstein, G. R. Boss, G. Hardie, and R. E. Shamu, Phys. Lett. **33B**, 465 (1970).

¹⁴O. Straume, G. Løvholden, and D. Burke, Nucl. Phys. **A266**, 390 (1976).

¹⁵H. L. Sharma, H. Taketani, and N. M. Hintz, Williams Laboratory of Nuclear Physics, University of Minnesota, Annual Report, 1974 (unpublished).

¹⁶A. Hoglund and S. G. Malmskog, Nucl. Phys. **A138**, 470 (1969).

¹⁷J. W. Ford, A. V. Ramayya, and J. J. Pinajian, Nucl. Phys. **A146**, 397 (1970).

¹⁸S. G. Nilsson, C. F. Tsang, A. Sobiczewski, Z. Szy-

manski, S. Wycech, C. Gustafson, I. Lamn, P. Möller, and B. Nilsson, Nucl. Phys. **A131**, 1 (1969).

¹⁹H. Taketani, M. Adachi, T. Hattori, T. Matsuzaki, and H. Nakayama, Phys. Lett. **63B**, 154 (1976).

²⁰S. Sen, J. Phys. A **6**, L45 (1973).

²¹J. R. Leigh, G. D. Dracoulis, M. G. Slocombe, and J. O. Newton, J. Phys. G **3**, 519 (1977).

²²G. D. Dracoulis, J. R. Leigh, A. Johnston, and C. Garrett, J. Phys. G **3**, 533 (1977).

²³G. D. Dracoulis and J. R. Leigh, J. Phys. G **2**, L87 (1976).

²⁴R. J. Dupzyk, C. M. Henderson, W. M. Buckley, G. L. Struble, R. G. Lanier, and L. G. Mann, Nucl. Instrum. Methods **153**, 53 (1978).

²⁵G. L. Struble, I. C. Oelrich, J. B. Carlson, L. G. Mann, and R. G. Lanier, Phys. Rev. Lett. **39**, 533 (1977).

²⁶R. G. Lanier, G. L. Struble, L. G. Mann, I. D. Proctor, and D. W. Heikkinen, Phys. Lett. **78B**, 217 (1978).

²⁷R. G. Lanier, L. G. Mann, G. L. Struble, I. D. Proctor, and D. W. Heikkinen, Phys. Rev. C **18**, 1609 (1978).

²⁸E. R. Flynn, S. Orbesen, J. D. Sherman, J. W. Sunier, and R. Woods, Nucl. Instrum. Methods **128**, 35 (1975).

²⁹A. Buyrn, Nucl. Data Sheets **14**, 471 (1975).

³⁰Agda Artina-Cohen, Nucl. Data Sheets **16**, 267 (1975).

³¹P. D. Kunz, Univ. of Colorado, Boulder, Colorado, computer code *dwck* (private communication).

³²C. M. Perey and F. G. Perey, At. Data Nucl. Data Tables **17**, 1 (1976).

³³E. R. Flynn, D. D. Armstrong, J. G. Beery, and A. G. Blair, Phys. Rev. **182**, 1113 (1969).

³⁴H. S. Song, J. J. Kolata, and J. V. Maher, Phys. Rev. C **16**, 1363 (1977).

³⁵W. Oelert, J. V. Maher, D. A. Sink, and M. J. Spisak, Phys. Rev. C **12**, 1495 (1975).

³⁶J. Kern and G. L. Struble, Nucl. Phys. **A286**, 371

- (1977).
- ³⁷T. von Egidy, W. Kaiser, W. Mampe, C. Hillebrand, W. Stöffl, R. G. Lanier, K. Mühlbauer, O. W. B. Schult, H. R. Koch, H. A. Baader, R. L. Mlekodaj, R. K. Sheline, E. B. Shera, J. Ungrin, P. T. Prokofiev, L. I. Simonova, M. K. Balodis, H. Seyfarth, B. Kardon, W. Delang, P. Göttel, D. Breitig, W. R. Kane, R. F. Casten, H. J. Scheerer, P. Glässl, E. Huenges, M. Löffler, H. Rösler, and H. K. Vonach, *Z. Phys.* A286, 341 (1978).
- ³⁸D. G. Burke, J. C. Waddington, and J. C. Tippet, *Phys. Lett.* 33B, 460 (1970).
- ³⁹L. A. Kroger and C. W. Reich, *Nucl. Data Sheets* 10, 429 (1973).
- ⁴⁰P. O. Tjøm and B. Elbek, *K. Dan. Vidensk. Selsk. Mat. Fys. Medd.* 36, No. 8 (1967).
- ⁴¹B. Nilsson, Computer code *cr* (private communication).
- ⁴²J. D. Immele and G. L. Struble, *Phys. Rev. C* 15, 1103 (1977).
- ⁴³B. B. Back, J. Bang, S. Bjørnhølm, J. Hattula, P. Kleinheinz, and J. R. Lien, *Nucl. Phys.* A222, 377 (1974).
- ⁴⁴The discrepancies noted between the calculated (d, t) spectra (Fig. 8) and angular distributions (Fig. 9) of this work and similar results given in Figs. 3 and 4 of Ref. 25 are due to differences in the single-particle energies used as well as off-setting errors in the DWBA calculations and in the experimental normalization of the reaction cross sections.